Electron Microscopic Visualization of Telomerase from *Euplotes aediculatus* Bound to a Model Telomere DNA†

Nicole Fouché,‡ Ian K. Moon,§ Brian R. Keppler,§ Jack D. Griffith,*,‡ and Michael B. Jarstfer§

Lineberger Comprehensive Cancer Center and Department of Biochemistry and Biophysics and School of Pharmacy, Division of Medicinal Chemistry, University of North Carolina, Chapel Hill, North Carolina 27599

Received February 14, 2006; Revised Manuscript Received May 12, 2006

ABSTRACT: Binding of the telomerase ribonucleoprotein from the ciliate *Euplotes aediculatus* to telomeric DNA in vitro has been examined by electron microscopy (EM). Visualization of the structures that formed revealed a globular protein complex that localized to the DNA end containing the *E. aediculatus* telomere consensus 3′-single-strand $T_4G_4T_4G_4T_4G_2$ overhang. Gel filtration confirmed that purified *E. aediculatus* telomerase is an active dimer in solution, and comparison of the size of the DNA-associated complex with apoferritin suggests that *E. aediculatus* telomerase binds to a single telomeric 3′-end as a dimer. Up to 43% of the telomerase−DNA complexes appeared by EM to involve tetramers or larger multimers of telomerase in association with two or more DNA ends. These data provide the first direct evidence that telomerase is a functional dimer and suggest that two telomerase ribonucleoprotein particles cooperate to elongate each *Euplotes* telomere in vivo.

Telomeres are nucleoprotein structures essential for chromosome stability in eukaryotes and regulation of the replicative lifespan of somatic cells. Encompassing the termini of all linear chromosomes, the telomeric DNA typically consists of long arrays of short tandem repeats (*1*) bound by specific DNA binding proteins, and which terminate in a single-stranded 3′-overhang (*2*, *3*). In the absence of telomerase or another mechanism for maintaining telomere length, most eukaryotic telomeres shorten by 50−200 nucleotides (nt)[1] during each cell cycle, due in part to the "end replication problem" that results from the inability of the lagging strand to be replicated to the very end of the chromosome (*4*, *5*).

The telomere-specific reverse transcriptase telomerase is able to maintain telomere length by using the single-strand overhang as a primer and a defined region of its integral RNA component as the template for the de novo synthesis of telomeric repeats (*6*, *7*). One unique feature of telomerase is its ability to add multiple copies of the repeat to a DNA substrate following a single initial binding event (*7*, *8*). This telomerase processivity depends on two types of translocation, type I or nucleotide addition processivity and type II or repeat addition processivity (*9*, *10*). Nucleotide addition processivity involves simultaneous movement of the RNA−DNA duplex relative to the active site after each nucleotide addition. Repeat addition processivity involves unpairing of the RNA−DNA hybrid after repeat addition, followed by translocation and re-alignment of the DNA substrate relative to the 3′-region of the RNA template. It has been proposed that telomerase can also associate with its DNA substrate via template-independent interactions that are regulated by a protein-dependent anchor site (*11*) and that these interactions may determine whether the product can remain bound to telomerase when released from the template site (*12*).

A feature of telomerase that may contribute to telomerase processivity is its ability to form dimers or multimers. Human TERT, the reverse transcriptase component of telomerase, and telomerase RNA form functionally cooperative oligomers in cell lysate or when reconstituted in vitro (*13*, *14*), and a mutation that weakens human telomerase RNA dimerization preferentially impairs type II processivity (*15*). *Tetrahymena thermophila* telomerase eluted from a gel filtration column at the size of a monomeric complex (*16*), but in *Saccharomyces cerevisiae*, the telomerase ribonucleoprotein particle (RNP) contains at least two active sites that both act as templates for DNA polymerization (*17*). Also, while glycerol gradient centrifugation of purified *Euplotes aediculatus* telomerase suggested an active RNP monomer in solution (*18*), gel filtration chromatography of *E. aediculatus* nuclear extracts revealed a functional telomerase complex in agreement with telomerase dimer formation (*19*). Indeed, *Euplotes crassus* telomerase complexes contain at least two active sites, and the telomerase catalytic subunit *Ec*TERT undergoes multimerization in vitro (*20*).

The existence of telomerase multimers suggests that two or more telomerase RNPs may cooperate during processive elongation to simultaneously extend one or more DNA substrates. Three models have thus been proposed for such cooperation in a coordinated dimer (*14*, *17*, *21*). The parallel extension model consists of two active sites within two different but associated telomerase RNPs simultaneously

† This work was supported in part by the Ellison Medical Foundation and National Institutes of Health Grants GM31819 and ES013773 awarded to J.D.G. as well as Grant MCB-0446019 from the National Science Foundation awarded to M.B.J.

* To whom correspondence should be addressed: Room 11-119, Lineberger Comprehensive Cancer Center, Mason Farm Road, University of North Carolina, Chapel Hill, NC 27599. Telephone: (919) 966-2151. Fax: (919) 966-3015. E-mail: jdg@med.unc.edu.

‡ Lineberger Comprehensive Cancer Center and Department of Biochemistry and Biophysics.

§ School of Pharmacy, Division of Medicinal Chemistry.

[1] Abbreviations: nt, nucleotides; RNP, ribonucleoprotein particle; EM, electron microscopy; TR, telomerase RNA; TERT, catalytic subunit of telomerase reverse transcriptase; BSA, bovine serum albumin.

10.1021/bi060313s CCC: $33.50
Published on Web 07/18/2006

extending two separate chromosome 3′-ends (*14*, *17*). It has been proposed that this type of coordinated extension could exist for elongation of both leading and lagging strand telomeres after DNA replication of sister chromatids. The template switching model evokes two catalytic sites within a dimer of telomerase acting sequentially during processive telomere synthesis to elongate a single telomere 3′-end (*14*). After addition of a repeat by the first telomerase RNP and upon translocation, the DNA substrate is re-aligned relative to the 3′-region of the RNA template within the second telomerase RNP. The DNA anchor site model proposes one telomerase RNP template stabilizing the interaction with a single telomere, while the other template is used for reverse transcription of the 3′-end (*21*). The template of one telomerase subunit is thus used primarily for substrate binding, presumably interacting with nucleotides upstream of the 3′-end of the DNA substrate, while the other is copied during telomere repeat addition. It is possible that these models are not mutually exclusive but that combinations of all three may exist, with the exact mechanics yet to be revealed.

E. aediculatus is a hypotrichous ciliate with a polyploid macronucleus containing millions of gene-sized chromosomes (*22*). The abundance of telomerase in each *E. aediculatus* cell thus makes it possible to routinely purify telomerase from crude extracts. *E. aediculatus* telomerase contains three subunits, including *Ea*TR (the 64 kDa RNA subunit), *Ea*TERT (the 123 kDa catalytic subunit), and a 43 kDa telomerase accessory protein (a La homologue that is important for nuclear retention and anchorage to an apparent end replication complex) (*18*, *23*). Together, these proteins form the functional ~230 kDa telomerase RNP in vivo.

Here, we used gel filtration and EM to examine purified *E. aediculatus* telomerase RNP and its binding to a model chromosome containing the *E. aediculatus* $T_4G_4T_4G_4T_4G_2$ consensus 3′-overhang (*2*, *24*). Size exclusion chromatography of telomerase compared to proteins with known molecular masses suggests that purified *E. aediculatus* telomerase is active as a dimer in solution. EM examination of binding reactions revealed mostly globular telomerase complexes bound to DNA. Comparison of particle size (projected area) to the globular protein apoferritin suggests that telomerase binds to telomeric 3′-ends as a dimer and that higher-order multimerization of these bound telomerases occurs, accordingly associating free DNA ends in vitro.

EXPERIMENTAL PROCEDURES

Growth of E. aediculatus and Preparation of Nuclear Extracts. *E. aediculatus* was grown under nonsterile conditions using Chlorogonium as the food source as previously described. Cultures were grown in 5 gal flasks with continuous aeration (*25*). Nuclei were isolated by sucrose cushion gradient centrifugation, and nuclear extracts were prepared by Dounce homogenization, as previously described (*24*).

Purification of E. aediculatus Telomerase. Telomerase was purified from nuclear extracts following the procedure described by Lingner and Cech (*18*). In short, nuclear extracts (15 mL from 1×10^9 cells) were chromatographed over a heparin−Sepharose column (Amersham Biosciences, Piscataway, NJ) using an increasing linear gradient of potassium glutamate, and the telomerase-containing fractions were pooled and concentrated using an Amicon stirred cell concentrator (Millipore, Billerica, MA). Telomerase was purified from these enriched fractions by affinity chromatography using a bait oligonucleotide, 5′-biotin-TAGACAC-CTGTTA-$(rmeG)_2$-$(rmeU)_4$-$(rmeG)_4$-$(rmeU)_4$-(rmeG)-3′, to trap telomerase onto Ultralink Neutravidin beads (Pierce Biotechnology, Inc., Rockford, IL). Telomerase was displaced by a chase oligonucleotide that is complementary to the bait, and the chase was removed by extensive dialysis against reaction buffer [20 mM Tris-acetate (pH 7.5), 10 mM $MgCl_2$, 50 mM potassium acetate, and 1 mM DTT] and concentrated. The quality of the purified telomerase was analyzed by silver staining of SDS−PAGE gels using standard procedures.

Gel Filtration. An AKTA FPLC system equipped with a Superdex 200 10/300 GL column (Amersham) was used. The column was equilibrated with 20 mM Tris-HCl (pH 7.5), 200 mM potassium acetate, 10 mM $MgCl_2$, 1 mM EDTA, 10% glycerol, and 1 mM DTT. Affinity-purified telomerase was injected, and the column was run at a rate of 0.4 mL/min at 4 °C. After 7 mL of void volume had passed through the column, 200 μL fractions were collected. The column was calibrated three times using the high-molecular mass calibration kit from Amersham ($R^2 = 0.9978$). Aldolase (158 kDa), ferritin (440 kDa), and thyroglobulin (669 kDa) were run at the same time on the Superdex 200 column, and their retention volumes were determined twice, in two separate runs, and fit to the curve $y = -148.18x + 2124.4$. The marker protein catalase (232 kDa) was run as a separate control to validate the calibration curve, since it has a retention volume that would be similar to that of a telomerase monomer.

Telomerase Quantification. The telomerase was quantified by analysis of the RNA subunit by solution hybridization with a ^{32}P-labeled probe for the *E. aediculatus* telomerase RNA. Quantities were normalized to RNA standards, and the amount of telomerase RNP was determined according to the calculation nanograms of RNP = nanograms of RNA/64 kDa × 230 kDa, where the mass of the RNA subunit is known to be 64 kDa and the mass of the telomerase RNP monomer is 230 kDa (*18*, *23*). We assumed the telomerase RNA was equimolar with the telomerase RNP monomer and that the majority of the RNA was contained within an intact telomerase complex.

DNA Manipulation. Model telomeres were synthesized by a modification of the method described by Stansel et al. (*26*). In short, the pRST5 plasmid (10 μg) was digested with BsmBI to generate a 5′-overhang with a TCCC sequence. The linearized DNA was incubated with the Klenow fragment of DNA polymerase 1, 33 μM dTTP, and 0.4 mM dCTP to create a blunt end on one side of the linear DNA. A 3′-overhang was generated by ligating either a telomeric DNA, Ea_CM_22 ($AGGGT_4G_4T_4G_4T_4G_2$), or nontelomeric DNA (AGGGATTGAATGACTACGAAGATGAA) oligomer onto linearized pRST5. Ligation reaction mixtures contained 5 μg of linearized pRST5, a 5-fold molar excess of 5′-phosphorylated oligonucleotide, T4 DNA ligase (200 units, New England Biolabs, Inc., Ipswich, MA), and T4 DNA ligase buffer (New England Biolabs) and were incubated at 25 °C for 30 min. Excess oligonucleotide was removed by size exclusion chromatography using Sephacryl-400 (Promega). DNA was deproteinized by the addition of

80 μg/mL proteinase K in 1% SDS followed by extraction with phenol and chloroform and concentration by ethanol precipitation. DNA was resuspended in 10 mM Tris-HCl (pH 7.6) and 1 mM EDTA to give a final concentration of ~20 ng/μL. Ligation efficiency was determined by treating ligated and unreacted linearized pRST5 with the Klenow fragment of DNA polymerase 1, [α-^{32}P]dGTP, and dATP and comparing the percent of incorporated dGTP. Typically, we achieved a ligation efficiency of 70%.

Telomerase Activity Assay and Catalyzed Extension of Model Telomeres. The ability of telomerase to extend telomere model DNAs was determined by a modification of a primer extension assay (*27*). Each 10 μL DNA extension assay contained 20 ng of DNA (see Figure 3B for details), 2 fmol of purified telomerase, 2 μCi of [α-^{32}P]dGTP (3000 Ci/mmol), 10 μM dGTP, 50 μM dTTP, 20 mM Tris-acetate (pH 7.5), 50 mM potassium acetate, 10 mM $MgCl_2$, and 1 mM DTT. Reaction mixtures were incubated at 25 °C for 30 min and reactions quenched by the addition of 20 mM Tris-acetate (pH 7.5), 10 mM EDTA, 1% SDS, and 80 μg/mL proteinase K. Extension products were recovered by ethanol precipitation and analyzed by electrophoresis on a 10 cm × 10 cm 4−12% acrylamide gradient gel containing 7 M urea. Dried gels were imaged by phosphorimaging (Molecular Storm 860) and quantified using ImagQuant version 5.2. The activity of telomerase in fractions eluted from the gel filtration column was similarly determined using a primer extension assay, where 50 μL of each fraction was reacted with 1 μM primer 5′-AATGAATGACTACGATTTT-3′ at 25 °C for 20 h. The radiolabeled primer [α-^{32}P]T_{10} was added to the quenching solution as a loading control, and extension products were analyzed by electrophoresis on a 20 cm × 20 cm denaturing PAGE gel.

Determination of the Primer K_m. K_m values for telomerase binding to the telomere model DNA Ea_CM_22 or to a short, single-stranded DNA primer, pEA22 (5′−$T_4G_4T_4G_4T_4G_2$), were determined by a DE81 filter binding assay. Affinity-purified telomerase (0.5 nM) was incubated with varying concentrations of primer (either pEA22 or Ea_CM_22), 50 μM dTTP, 10 μM dGTP, and 0.33 μM [α-^{32}P]dGTP (3000 Ci/mmol) in telomerase reaction buffer for 30 min at 25 °C. Reactions were quenched by the addition of 50 mM EDTA and mixtures spotted onto DE81 filter paper. Unincorporated [α-^{32}P]dGTP was washed away with 0.5 M sodium phosphate (pH 7.0). Filters were counted by liquid scintillation counting, and the data were corrected by the subtraction of background binding to the filter using a telomerase negative reaction. Data were fit to the Michaelis−Menten equation using Sigma Plot.

Electron Microscopy. Model telomeric DNA was diluted to 1 μg/mL in 10 mM HEPES (pH 7.5), 50 mM potassium acetate, 8% PEG, and 2 mM magnesium acetate followed by addition of *E. aediculatus* telomerase to a concentration of 0.7 μg/mL for 10 min at 37 °C. Proteins were fixed onto the DNA with 0.6% glutaraldehyde, and the mixtures were filtered through 2 mL columns of Bio-Gel A-5m (Bio-Rad Laboratories, Inc., Hercules, CA) that had been equilibrated with 0.01 M Tris-HCl (pH 7.6) and 0.1 mM EDTA. Addition of spermidine to a concentration of 2.5 mM and $MgCl_2$ to a concentration of 1 mM allowed adsorption of the sample onto copper grids supporting thin, glow-charged carbon foils. The samples were washed stepwise with 25, 50, 75, and 100% ethanol for 5 min followed by air drying and rotary shadowcasting with tungsten (*28*). An FEI Tecnai 12 electron microscope was used at an accelerating voltage of 40 kV to photograph images on plate film or a Gatan 4K × 4K CCD camera. Micrographs for publication were captured from plate film negatives using a Nikon SMZ1000 digital camera, and morphometry measurements were taken using ImageJ version 1.29 (National Institutes of Health).

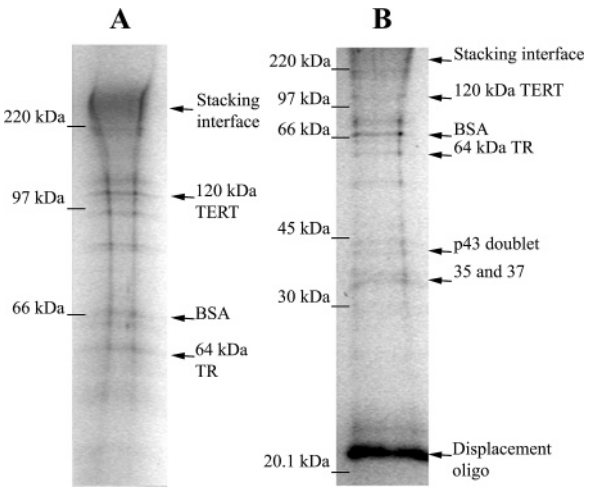

FIGURE 1: Affinity-purified telomerase fractions were separated on 10% polyacrylamide gels and stained with silver. The sample in lane A was run twice as long as the sample in lane B. Sizes of molecular mass markers that were run with the samples are given in kilodaltons at the left. Locations of known polypeptides, DNA, and RNA are indicated (arrows). The interface between the stacking and separating gels (stacking interface) is also indicated as a possible site of protein precipitation.

RESULTS

E. aediculatus telomerase was purified by the method of Lingner and Cech (*18*). The total fold purification of the affinity-purified fractions could not be determined due to very low yields as well as the large amount of BSA used in the purification procedure. However, we estimated the telomerase to be approximately 50% pure, as reported previously for the purification of a much larger culture with much higher yields (*18*).

The quality of the purified telomerase was analyzed by silver staining of SDS−PAGE gels (Figure 1). Bands corresponding to all known *E. aediculatus* subunits were seen (120 kDa TERT, 64 kDa TR, and p43 doublet) as well as bands for known polypeptide contaminants (BSA and polypeptides 35 and 37) (*18*). The interface between the stacking and separating gels (stacking interface) is shown as a possible site of protein precipitation. Additional bands were seen that were likely polypeptide contaminants, but because samples were very dilute, it was not possible to determine the stoichiometry of these contaminating proteins with respect to telomerase. Nevertheless, these proteins did not appear to interfere with telomerase activity, which was robust in all assays, and because there was no protein observed in the binding of EM to nontelomeric DNA templates, we do not believe that these contaminants interfered with the telomerase EM binding experiments (results discussed below). Indeed, when Hammond et al. cross-linked partially purified *E. aediculatus* to ^{32}P-radiolabeled single-stranded telomeric DNA, only one type of protein−primer product was observed (*29*).

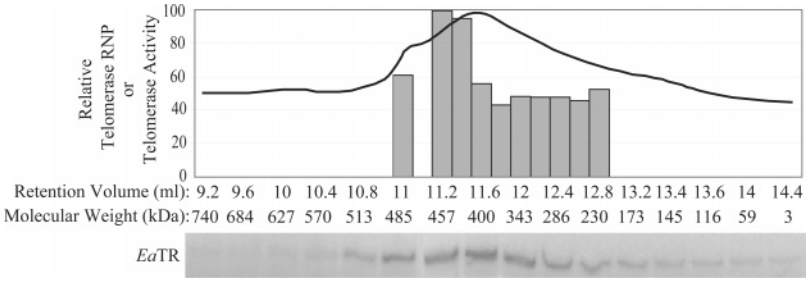

FIGURE 2: Telomerase profile which suggests a dimer in solution. Elution profile of affinity-purified *Euplotes* telomerase chromatographed on a Superdex 200 gel filtration column. The amount of telomerase (line graph) in each fraction collected was determined by detection of the RNA subunit *Ea*TR. Fractions that contained telomerase were then assayed for telomerase activity (bar graph), as described in Experimental Procedures. Only fractions with activity above background are shown. Amounts and activities are shown relative to the highest value, which was set to 100%.

The oligomeric state of the telomerase was determined by gel filtration on a Superdex 200 column. The fractions were assayed for *E. aediculatus* telomerase RNA (*Ea*TR) content and for telomerase activity (Figure 2). The retention volume of telomerase was compared to that of four marker proteins with known molecular masses. The *Ea*TR content peaked with a retention volume of 11.6 mL, corresponding to an approximate molecular mass of 400 kDa, whereas the telomerase activity peaked with a retention volume of 11.2 mL, corresponding to an approximate molecular mass of 457 kDa. If the shape of the telomerase particle does not greatly deviate from spherical, then this result would be consistent with the predicted mass of a telomerase dimer of ~460 kDa (the molecular mass of telomerase is ~230 kDa), a result that is in agreement with gel filtration chromatography of *E. aediculatus* nuclear extracts carried out previously by Aigner et al. (*19*). The slight offset between the peak RNA content and the peak telomerase activity could then be due to some dissociation of telomerase subunits during the gel filtration experiments, which could also account for the lower activity of the fractions with a lower apparent molecular mass. These data suggest, therefore, that *E. aediculatus* telomerase may be an active dimer in solution.

A synthetic model telomere was prepared by linearizing the pRST5 plasmid to generate a 3.5 kb DNA with one end terminating in 550 bp of TTAGGG repeats and a 5′-overhang. A single-strand oligonucleotide was ligated to this end to generate a 22 nt 3′-overhang consisting of the *E. aediculatus* $T_4G_4T_4G_4T_4G_2$ repeat (Ea_CM_22, Figure 3A) (Experimental Procedures). A control DNA with a nontelomeric overhang was similarly prepared using the random sequence single-strand oligonucleotide ATTGAATGACTACGAAGATGAA. In these reactions, we routinely achieved a ligation efficiency of 65−70%.

To determine if the model Ea_CM_22 telomere could act as a telomerase primer, we examined the ability of telomerase to extend the model DNA using [α-^{32}P]dGTP in the reaction mixture. Reaction products were analyzed by electrophoresis on an acrylamide gradient gel for the incorporation by telomerase of [α-^{32}P]dGTP into the substrate DNAs. We found that Ea_CM_22 was an efficient substrate while linear pRST5 DNA that did not contain a telomeric overhang was not a substrate (Figure 3B) and determined that the K_m for binding of telomerase to Ea_CM_22 was 4 nM as compared to a value of 14 nM for a 22 nt primer used as a control, which is comparable to the reactivity of primers with any of the possible permutations of the telomeric sequence (*27*, *30*).

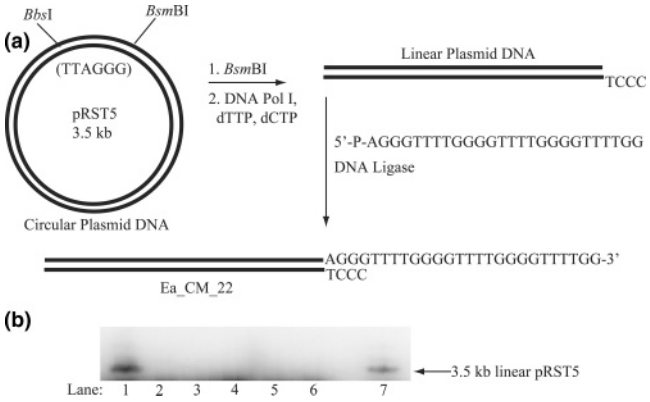

FIGURE 3: Telomerase can extend a model chromosome. (A) Synthesis of a *Euplotes* model telomere DNA (Ea_CM_22). Details of the enzymatic steps are in Experimental Procedures. (B) Affinity-purified telomerase was incubated with dTTP, [α-^{32}P]dGTP, and either Ea_CM_22 (lane 1), Ea_CM_22 and RNase A (lane 2), linear pRST5 with a nontelomeric end (lane 3), linear pRST5 with a nontelomeric end and RNAse (lane 4), linear pRST5 (lane 5), or linear pRST5 with RNase (lane 6). Lane 7 contained a marker for linear pRST5.

Purified *E. aediculatus* telomerase was incubated with the 3.5 kb model telomere DNA Ea_CM_22 or the linear control DNA with the random sequence overhang. The reaction conditions were consistent with those used to show that the purified telomerase was able to extend the model telomere but were varied slightly to achieve the best conditions for visualizing protein−DNA complexes by EM. Alternative permutations of the telomerase repeat sequence were not studied because it has been previously shown that, while telomerase processivity is affected, telomerase is able to bind to and utilize primers containing very few or no telomeric nucleotides at the 3′-end (*31*). Thus, binding reactions were performed for different reaction times (from 1 to 20 min) at varying temperatures (4, 25, and 37 °C) and protein:DNA molar ratios (from 5:1 to 14:1) and in the presence or absence of PEG, a molecular crowding agent. Optimum conditions included using a 7.5:1 molar ratio of telomerase to DNA in the presence of 8% PEG for 10 min at 37 °C. The resulting complexes were fixed with glutaraldehyde and examined by EM.

When *E. aediculatus* telomerase was incubated with the model telomere and prepared for EM, an array of telomerase−DNA complexes were observed (Figure 4). The most common species consisted of a single model telomere DNA bound at one end by telomerase (Figure 4A−C). Also present were complexes containing two or more model telomeres,

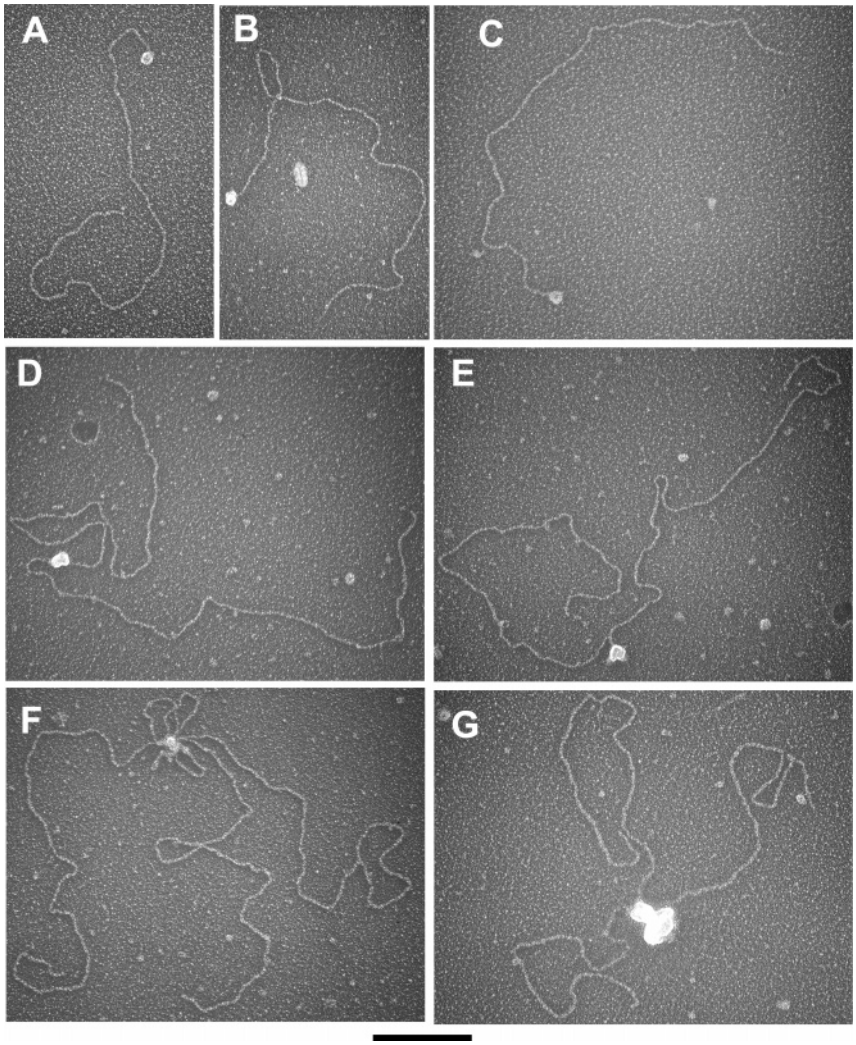

FIGURE 4: Visualization of *Euplotes* telomerase bound to a model telomere substrate. *E. aediculatus* telomerase was incubated with a 3 kb model telomere DNA (Figure 3) and then prepared for EM by being fixed with glutaraldehyde, mounted on carbon-coated EM grids, and rotary shadowcasted with tungsten (Experimental Procedures). Telomerase bound at one end of the model telomere (A−C). Examples of two (D and E) or three (F and G) model telomere DNAs bound together at one end by a telomerase complex. Images are shown in reverse contrast. The bar is equivalent to 500 bp.

Table 1: Percent of Model Telomere DNAs Bound at Their End by a Telomerase Complex

reaction	no. of molecules counted	end-bound complexes (%)
1	104	52
2	109	47
3	45	40
4	43	42
5	54	50
average	71	46

each with one end synapsed to the other DNA by a large commonly bound telomerase complex (Figure 4D−G). Less frequently seen were DNA molecules containing one or more internally bound protein complexes (not shown).

Five separate reactions were scored with an average of 71 molecules counted per experiment (Table 1). In total, 46% of all telomere model DNAs showed a telomerase complex bound at one end.

When the nontelomeric overhang was employed, only 4% of the ends showed a protein bound. Thus, the telomeric 3′-end of the model telomere is bound specifically by one or more telomerase molecules. Quantification of the protein-bound DNA molecules revealed an average of 45% with a telomerase complex bound to a single model telomere end, whereas 22 and 21% had two and three DNAs, respectively, with their ends associated through a large telomerase complex, likely a telomerase oligomer. Telomerase was observed bound nonspecifically to internal DNA sequences within the model telomere in 12% of the DNAs. Occasionally, very large DNA−protein aggregates were seen and were not included in the scoring. Using a lower concentration of telomerase in the binding reactions alleviated this problem somewhat, although optimum conditions for binding required that the telomerase concentration not be too low.

From these observations, we conclude that *E. aediculatus* telomerase binds to the 3′-consensus overhang of the model telomere and that it is also capable of self-association, consequently bringing two or more DNA ends together in vitro. This, however, should not necessarily be viewed as evidence that telomerase is able to synapse two chromosome ends in vivo.

The degree of oligomerization of the bound telomerase complexes was determined using a variation of a method used in our previous studies (*32*, *33*). A large protein standard of known mass is mixed with the sample, and the size

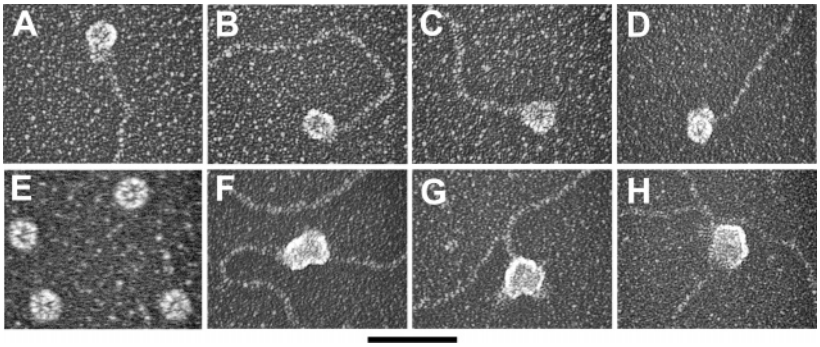

FIGURE 5: Estimation of the oligomeric state of DNA-bound telomerase by direct size comparison. Telomerase complexes at the ends of single model telomeres (A−D) or joining two model telomeres (F−H) were compared to apoferritin particles (E). The telomerase DNA complexes and apoferritin were prepared for EM side by side on separate EM supports. Images are shown in reverse contrast, and the bar is equivalent to 500 bp.

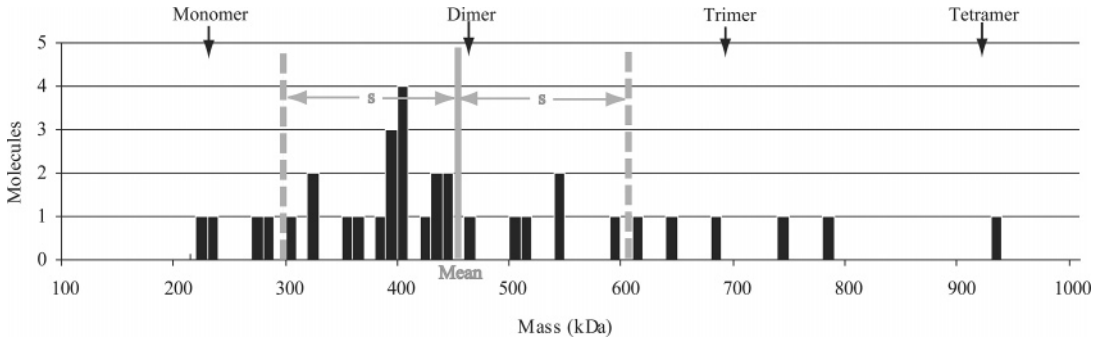

FIGURE 6: Histogram of the calculated mass of telomerase at the end of a single model telomere. The calculated mass values derived from measurements of the projected areas of telomerase complexes bound to the end of a single model telomere DNA are shown. The mean calculated mass value (solid gray line) was 447 kDa with a standard deviation of 151 kDa (s, dotted gray lines). Molecular masses of a monomer (230 kDa), dimer (460 kDa), trimer (690 kDa), and tetramer (920 kDa) of telomerase are denoted with arrows.

(projected area in the micrographs) of the standard is compared to the projected area of the protein bound to the DNA. If the standard and sample are similar in size and shape, molecular mass estimates that can differentiate with certainty between different oligomeric states of the protein bound to DNA can be derived. In this study, since there was a significant amount of free telomerase in the background on the grids, the molecular mass standard was adsorbed on separate grids and the standard and sample were processed for EM side by side. This can be expected to add some but not a significant additional measurement error.

The telomerase complexes on DNA appeared mostly globular, and inspection showed that apoferritin (443 kDa) was close in size (projected area) to the class of telomerase particles most frequently seen at the ends of a single model telomere DNA, suggesting that these particles may consist of telomerase dimers. Photographs of fields of apoferritin molecules were taken, and the mean projected area of 30 examples was measured (Figure 5E). The average projected area of the apoferritin was set to an arbitrary value of 100 units. On the basis of the mass of a telomerase monomer, the predicted projected area relative to apoferritin should be 64 units as determined by the formula: mass of telomerase/mass of apoferritin = (area of telomerase/area of apoferritin)$^{3/2}$.

Similarly, the predicted projected areas of a dimer, trimer, tetramer, and pentamer would be 102, 134, 162, and 188 units, respectively. These sizes were then compared to measurements of projected areas of telomerase complexes bound to the end of a single model telomere DNA (Figure 5A−D). A histogram representing the calculated mass derived from such measurements is shown in Figure 6. The mean projected area of the complex was thus 101 ± 23 units, and the mean calculated mass value was 455 ± 160 kDa (n = 34). Assuming the telomerase complex binds only to the consensus 3′-overhang, we subtracted ~8.6 kDa for the single-strand $[T_4G_4]_2$TTTTGG sequence which resulted in a mass of 447 ± 151 kDa. Although the distributions may have been broadened by the slightly oblong shape of the telomerase and thus by variations in projections of the telomerase particles, these data suggest that the telomere end was most commonly bound by a dimer of telomerase. This finding is consistent with the size of telomerase determined by gel filtration here and previously reported (*19*).

For the class of telomerase particles bound at the junction of two model telomeres, the protein mass was frequently much larger than that of apoferritin. The projected areas of a subset (n = 19) of the smallest particles were measured, however, revealing a broad distribution of calculated mass values (Figure 5F−H). When compared to that of apoferritin (set to 100 units), the mean projected area of these particles was 176 ± 64 units. After subtraction of ~17 kDa for the DNA content, this resulted in a mean calculated mass of 1061 ± 569 kDa. Although this value is sufficiently broad to encompass a dimer (460 kDa) or trimer (690 kDa) of telomerase, the data seem more likely to suggest that, at a minimum, two dimers of telomerase, each associated with a model telomere, bind to form a tetramer (920 kDa) in vitro. Indeed, for this class of particles, one could occasionally distinguish a region of separation between two globular particles, each the size of a dimer, that is consistent with a dimer of dimers (Figure 4D−G).

DISCUSSION

In this study, *E. aediculatus* telomerase was isolated from nuclear extracts using affinity chromatography with an antisense oligonucleotide. Although electrophoretic analysis of fractions revealed several contaminants, these did not interfere with telomerase activity, which was robust, or with our EM binding experiments, as seen by the lack of protein binding to control DNA templates.

The molecular mass of telomerase, determined by gel filtration, was consistent with the mass of a dimer. When the telomerase particle was visualized by EM, its shape was seen to be mostly globular, and inspection of the telomerase bound to its substrate showed that it bound predominantly as a dimer. Taken together, we find these observations to be convincing evidence that *E. aediculatus* telomerase dimerizes in solution and that it binds to telomeric DNA as a multimer, most likely as a dimer.

It was also shown by EM and a modified primer extension assay that telomerase specifically binds to and extends the consensus telomeric 3′-overhang in vitro. Further, when end-to-end pairing of two DNA molecules occurred, the telomerase complex was likely a tetramer or larger oligomer.

These findings are consistent with a model of processive telomere reverse transcription consisting of two cooperating telomerases that bind to and extend a single DNA substrate. The data do not support an obligate parallel extension model of telomerase cooperation, where two active sites within two different but associated telomerase RNPs simultaneously extend two separate chromosome 3′-ends (*14*, *17*), although it is still possible that two dimers of telomerase can coordinate to extend two separate but adjacent chromosome ends, such as sister chromatids.

Rivera et al. showed that a dimeric human telomerase can processively utilize a single template (*34*), which argues against the template switching model in humans, where the two catalytic sites would act sequentially to elongate a single telomere 3′-end (*14*). Nevertheless, *Euplotes* is an evolutionarily very distant species, and it is still possible that the template switching model or the DNA anchor site model, where one telomerase RNP template anchors the dimer while the other template is used for reverse transcription (*21*), or combinations of these models may exist.

This study is the first visualization of intact telomerase bound to a DNA substrate, and it provides the first direct proof of telomerase RNP multimerization in *E. aediculatus*.

ACKNOWLEDGMENT

We are grateful to Funda Sar for her help with the gel filtration experiments and Sezgin Özgür for useful suggestions.

REFERENCES

1. Meyne, J., Ratliff, R. L., and Moyzis, R. K. (1989) Conservation of the human telomere sequence $(TTAGGG)_n$ among vertebrates, *Proc. Natl. Acad. Sci. U.S.A. 86*, 7049−53.
2. Klobutcher, L. A., Swanton, M. T., Donini, P., and Prescott, D. M. (1981) All gene-sized DNA molecules in four species of hypotrichs have the same terminal sequence and an unusual 3′ terminus, *Proc. Natl. Acad. Sci. U.S.A. 78*, 3015−9.
3. Henderson, E. R., and Blackburn, E. H. (1989) An overhanging 3′ terminus is a conserved feature of telomeres, *Mol. Cell. Biol. 9*, 345−8.
4. Watson, J. D. (1972) Origin of concatemeric T7 DNA, *Nat. New Biol. 239*, 197−201.
5. Olovnikov, A. M. (1973) A theory of marginotomy. The incomplete copying of template margin in enzymic synthesis of polynucleotides and biological significance of the phenomenon, *J. Theor. Biol. 41*, 181−90.
6. Lingner, J., Hughes, T. R., Shevchenko, A., Mann, M., Lundblad, V., and Cech, T. R. (1997) Reverse transcriptase motifs in the catalytic subunit of telomerase, *Science 276*, 561−7.
7. Greider, C. W., and Blackburn, E. H. (1985) Identification of a specific telomere terminal transferase activity in *Tetrahymena* extracts, *Cell 43*, 405−13.
8. Greider, C. W. (1991) Telomerase is processive, *Mol. Cell. Biol. 11*, 4572−80.
9. Lue, N. F. (2004) Adding to the ends: What makes telomerase processive and how important is it? *BioEssays 26*, 955−62.
10. Peng, Y., Mian, I. S., and Lue, N. F. (2001) Analysis of telomerase processivity: Mechanistic similarity to HIV-1 reverse transcriptase and role in telomere maintenance, *Mol. Cell 7*, 1201−11.
11. Harrington, L. A., and Greider, C. W. (1991) Telomerase primer specificity and chromosome healing, *Nature 353*, 451−4.
12. Collins, K. (1999) Ciliate telomerase biochemistry, *Annu. Rev. Biochem. 68*, 187−218.
13. Beattie, T. L., Zhou, W., Robinson, M. O., and Harrington, L. (2001) Functional multimerization of the human telomerase reverse transcriptase, *Mol. Cell. Biol. 21*, 6151−60.
14. Wenz, C., Enenkel, B., Amacker, M., Kelleher, C., Damm, K., and Lingner, J. (2001) Human telomerase contains two cooperating telomerase RNA molecules, *EMBO J. 20*, 3526−34.
15. Moriarty, T. J., Marie-Egyptienne, D. T., and Autexier, C. (2004) Functional organization of repeat addition processivity and DNA synthesis determinants in the human telomerase multimer, *Mol. Cell. Biol. 24*, 3720−33.
16. Bryan, T. M., Goodrich, K. J., and Cech, T. R. (2003) *Tetrahymena* telomerase is active as a monomer, *Mol. Biol. Cell 14*, 4794−804.
17. Prescott, J., and Blackburn, E. H. (1997) Functionally interacting telomerase RNAs in the yeast telomerase complex, *Genes Dev. 11*, 2790−800.
18. Lingner, J., and Cech, T. R. (1996) Purification of telomerase from *Euplotes aediculatus*: Requirement of a primer 3′ overhang, *Proc. Natl. Acad. Sci. U.S.A. 93*, 10712−7.
19. Aigner, S., Postberg, J., Lipps, H. J., and Cech, T. R. (2003) The *Euplotes* La motif protein p43 has properties of a telomerase-specific subunit, *Biochemistry 42*, 5736−47.
20. Wang, L., Dean, S. R., and Shippen, D. E. (2002) Oligomerization of the telomerase reverse transcriptase from *Euplotes crassus*, *Nucleic Acids Res. 30*, 4032−9.
21. Kelleher, C., Teixeira, M. T., Forstemann, K., and Lingner, J. (2002) Telomerase: Biochemical considerations for enzyme and substrate, *Trends Biochem. Sci. 27*, 572−9.
22. Prescott, D. M. (1994) The DNA of ciliated protozoa, *Microbiol. Rev. 58*, 233−67.
23. Aigner, S., Lingner, J., Goodrich, K. J., Grosshans, C. A., Shevchenko, A., Mann, M., and Cech, T. R. (2000) *Euplotes* telomerase contains an La motif protein produced by apparent translational frameshifting, *EMBO J. 19*, 6230−9.
24. Lingner, J., Hendrick, L. L., and Cech, T. R. (1994) Telomerase RNAs of different ciliates have a common secondary structure and a permuted template, *Genes Dev. 8*, 1984−98.
25. Swanton, M. T., Heumann, J. M., and Prescott, D. M. (1980) Gene-sized DNA molecules of the macronuclei in three species of hypotrichs: Size distributions and absence of nicks. DNA of ciliated protozoa. VIII, *Chromosoma 77*, 217−27.
26. Stansel, R. M., de Lange, T., and Griffith, J. D. (2001) T-Loop assembly in vitro involves binding of TRF2 near the 3′ telomeric overhang, *EMBO J. 20*, 5532−40.
27. Jarstfer, M. B., and Cech, T. R. (2002) Effects of nucleotide analogues on *Euplotes aediculatus* telomerase processivity: Evidence for product-assisted translocation, *Biochemistry 41*, 151−61.
28. Griffith, J. D., and Christiansen, G. (1978) Electron microscope visualization of chromatin and other DNA-protein complexes, *Annu. Rev. Biophys. Bioeng. 7*, 19−35.
29. Hammond, P. W., Lively, T. N., and Cech, T. R. (1997) The anchor site of telomerase from *Euplotes aediculatus* revealed by photo-cross-linking to single- and double-stranded DNA primers, *Mol. Cell. Biol. 17*, 296−308.

30. Hammond, P. W., and Cech, T. R. (1997) dGTP-dependent processivity and possible template switching of euplotes telomerase, *Nucleic Acids Res. 25*, 3698−704.
31. Hammond, P. W., and Cech, T. R. (1998) *Euplotes* telomerase: Evidence for limited base-pairing during primer elongation and dGTP as an effector of translocation, *Biochemistry 37*, 5162−72.
32. Griffith, J., Bianchi, A., and de Lange, T. (1998) TRF1 promotes parallel pairing of telomeric tracts in vitro, *J. Mol. Biol. 278*, 79−88.
33. Allen, D. J., Makhov, A., Grilley, M., Taylor, J., Thresher, R., Modrich, P., and Griffith, J. D. (1997) MutS mediates heteroduplex loop formation by a translocation mechanism, *EMBO J. 16*, 4467−76.
34. Rivera, M. A., and Blackburn, E. H. (2004) Processive utilization of the human telomerase template: Lack of a requirement for template switching, *J. Biol. Chem. 279*, 53770−81.

BI060313S